Cancer Therapy: Preclinical

Clinical Cancer Research

Pretargeted Radioimmunotherapy Using Genetically Engineered Antibody-Streptavidin Fusion Proteins for Treatment of Non-Hodgkin Lymphoma

Steven I. Park[1], Jaideep Shenoi[2,3], Shani M. Frayo[2], Donald K. Hamlin[4], Yukang Lin[2], D. Scott Wilbur[4], Patrick S. Stayton[5], Nural Orgun[2], Mark Hylarides[2], Franz Buchegger[6], Aimee L. Kenoyer[2], Amanda Axtman[2], Ajay K. Gopal[2,3], Damian J. Green[2,3], John M. Pagel[2,3], and Oliver W. Press[2,3]

Abstract

Purpose: Pretargeted radioimmunotherapy (PRIT) using streptavidin (SAv)-biotin technology can deliver higher therapeutic doses of radioactivity to tumors than conventional RIT. However, "endogenous" biotin can interfere with the effectiveness of this approach by blocking binding of radiolabeled biotin to SAv. We engineered a series of SAv FPs that downmodulate the affinity of SAv for biotin, while retaining high avidity for divalent DOTA-bis-biotin to circumvent this problem.

Experimental Design: The single-chain variable region gene of the murine 1F5 anti-CD20 antibody was fused to the wild-type (WT) SAv gene and to mutant SAv genes, Y43A-SAv and S45A-SAv. FPs were expressed, purified, and compared in studies using athymic mice bearing Ramos lymphoma xenografts.

Results: Biodistribution studies showed delivery of more radioactivity to tumors of mice pretargeted with mutant SAv FPs followed by ^{111}In-DOTA-bis-biotin [6.2 $\pm$ 1.7% of the injected dose per gram (%ID/gm) of tumor 24 hours after Y43A-SAv FP and 5.6 $\pm$ 2.2%ID/g with S45A-SAv FP] than in mice on normal diets pretargeted with WT-SAv FP (2.5 $\pm$ 1.6%ID/g; $P = 0.01$). These superior biodistributions translated into superior antitumor efficacy in mice treated with mutant FPs and ^{90}Y-DOTA-bis-biotin [tumor volumes after 11 days: 237 $\pm$ 66 mm^3 with Y43A-SAv, 543 $\pm$ 320 mm^3 with S45A-SAv, 1129 $\pm$ 322 mm^3 with WT-SAv, and 1435 $\pm$ 212 mm^3 with control FP ($P < 0.0001$)].

Conclusions: Genetically engineered mutant-SAv FPs and bis-biotin reagents provide an attractive alternative to current SAv-biotin PRIT methods in settings where endogenous biotin levels are high. *Clin Cancer Res; 17(23); 7373–82. ©2011 AACR.*

Introduction

Despite advances in the management of lymphoma, fewer than 60% of patients with aggressive non-Hodgkin lymphomas (NHL) and fewer than 5% of patients with indolent lymphomas can be cured with conventional chemotherapy (1–3). The remaining patients eventually relapse, and the disease becomes progressively more chemotherapy resistant. This does not preclude the therapeutic benefit of radiation therapy; however, because lymphoma cells remain highly susceptible to even low doses of radiation regardless of their inherent resistance to chemotherapeutic drugs. For this reason, radioimmunotherapy (RIT) has emerged as a promising treatment option for NHL. RIT has yielded excellent overall response rates of 50% to 80%, with complete response rates of 20% to 40% in patients with relapsed or refractory indolent lymphoma treated with iodine-131 (^{131}I) tositumomab (Bexxar, GlaxoSmithKline) or yttrium-90 (^{90}Y) ibritumomab tiuxetan (Zevalin, Spectrum; refs. 4–7). Nevertheless, most patients treated with conventional doses of RIT eventually relapse even after favorable initial responses. Dose escalation of RIT to myeloablative levels with stem-cell support significantly reduces the risk of relapse by delivering potentially curative radiation doses to tumor sites. However, this approach has been associated with significant treatment-related morbidity and mortality (8–10).

One strategy for delivering higher, potentially curative, radiation doses to tumors involves a multistep "pretargeting" method. The major cause of dose-limiting toxicities in conventional RIT is due to the slow clearance of unbound radiolabeled antibodies (Ab) from the circulation with

Authors' Affiliations: [1]Department of Medicine, University of North Carolina, Chapel Hill, North Carolina; [2]Clinical Research Division, Fred Hutchinson Cancer Research Center; Departments of [3]Medicine, [4]Radiation Oncology, and [5]Bioengineering, University of Washington, Seattle, Washington; and [6]University Hospital of Lausanne, Lausanne, Switzerland

Note: Supplementary data for this article are available at Clinical Cancer Research Online (http://clincancerres.aacrjournals.org/).

S.I. Park and J. Shenoi contributed equally to this work.

Corresponding Author: Oliver W. Press, Fred Hutchinson Cancer Research Center, 1100 Fairview Ave., N, M/S D3-395, Seattle, WA 98109. Phone: 206-667-1864; Fax: 206-667-1874; E-mail: press@u.washington.edu

doi: 10.1158/1078-0432.CCR-11-1204

Translational Relevance

Conventional radioimmunotherapy (RIT) induces long-term durable remissions in more than 50% of patients with relapsed or refractory indolent non-Hodgkin lymphoma.

Our research goal is to optimize RIT using a multistep pretargeted RIT scheme (PRIT) employing genetically engineered mutant-streptavidin fusion proteins and bis-biotin reagents that provide an attractive alternative to current methods. This molecular engineering approach is particularly attractive in clinical settings where high endogenous biotin levels prevail due to dietary intake of this vitamin, leading to diminished efficacy of standard streptavidin/biotin reagents.

We anticipate that this approach will result in superior efficacy compared with both conventional RIT and current PRIT approaches. If the results are promising, we anticipate eventually translating this approach into phase I/II clinical studies of PRIT for patients with relapsed B-cell lymphomas.

resultant high levels of background radioactivity in normal tissues (11–13). Pretargeted radioimmunotherapy (PRIT) dissociates the slow distribution phase of the Ab molecule from administration of the therapeutic radionuclide. This approach permits the tumor-reactive Ab to localize and accumulate at tumor sites without subjecting the rest of the body to nonspecific irradiation from circulating radiolabeled Ab (14–17). After maximal accumulation of Ab in the tumor, a small molecular weight radioactive moiety, which has high affinity for the tumor-reactive Ab is administered. This second reagent penetrates tumors rapidly due to its small size. Excess unbound molecules of the second radioactive reagent are also rapidly cleared from the blood and excreted in the urine due to their small size. To facilitate this process, a "clearing agent" (CA) may be injected before the radiolabeled small molecule to enhance elimination of the unbound Ab from the bloodstream thus preventing it from complexing with the radiolabeled small molecule in the circulation.

Preclinical data have shown that streptavidin (SAv)-biotin pretargeting strategies can dramatically increase the tumor-to-normal organ ratio of delivered radioactivity by 10- to 100-fold (16–18). Pilot clinical trials have also shown promising results in both solid tumor and lymphoma models, though the outcomes were not as dramatic as those observed in preclinical studies (19–22). Suboptimal responses observed in the pilot clinical trials may be partially attributable to the presence of competing endogenous biotin in patient serum, derived from dietary sources. Biotin is present in blood and tissues at sufficient concentrations to irreversibly block the biotin-binding sites of SAv and may impair its efficacy in pretargeting applications (21, 23). In preclinical studies, mice may be fed a biotin-deficient diet for several days prior to the therapy to reduce the endogenous biotin concentration in serum. In contrast, biotin-depletion in human clinical trials is more problematic due to the ubiquitous presence of this vitamin in all common foods, patient noncompliance, and concerns over complications attributable to biotin deficiency. Although the serum concentration of biotin present in humans is somewhat lower than in mice, endogenous biotin remains a significant concern, particularly because the liver acts as a storage and release reservoir for biotin (24). Strategies that avoid the blocking of the biotin-binding sites of SAv by endogenous biotin may therefore offer therapeutic advantages. To address this issue, Stayton and colleagues produced a large library of SAv variants by site-directed mutagenesis directed at the SAv-binding pocket (Supplementary Table S1), covering a wide range of K_a and K_{off} properties (25–26). Along with the engineering of SAv mutants, divalent bis-biotin ligands were designed to effectively engage 2 adjacent biotin-binding sites of SAv mutants, thus overcoming the competitive binding by endogenous biotin (27–29). The lower affinities and faster biotin off-rates of the SAv mutants allow exchange of prebound endogenous biotin, although the dual binding of the bis-biotin ligand results in a striking avidity effect and essentially irreversible capture of the modified divalent ligand (27, 30–32). In this manuscript, we describe the synthesis and characterization of 2 SAv mutant fusion proteins (FP), S45A-SAv and Y43A-SAv. The FPs were selected based on previous kinetic studies suggesting they were the most promising candidates that would allow exchange of prebound monovalent endogenous biotin while retaining sufficiently high affinity to efficiently capture radiolabeled divalent bis-biotin ligands (27, 29). We report here the blood clearance of the mutant-SAv FPs using a standard monovalent biotin CA or a novel bivalent biotin CA, specifically designed for this application. Finally, we compare the targeting, biodistributions, and therapeutic efficacy of PRIT strategies utilizing either conventional wild type (WT)-SAv and biotin or mutant-SAv and bis-biotin reagent combinations.

Materials and Methods

Cell culture

The human Ramos Burkitt lymphoma cell line was obtained from the American Type Culture Collection (ATCC). Cell lines were maintained in log phase growth in RPMI 1640 medium supplemented with 10% heat-inactivated fetal calf serum in a 5% CO_2 incubator. Cell viability exceeded 95% by trypan blue exclusion.

WT-SAv FP and mutant-SAv FPs

The development of the 1F5-WT-SAv FP has been previously described (33–35). Briefly, the process involved fusion of the single-chain variable regions (scFv) of the murine anti-CD20 1F5 Ab to the full length genomic SAv of *Streptomyces avidinii* WT gene to obtain the 1F5$(scFv)_4$SAv fusion gene. This gene construct was modified by PCR-based site-directed mutagenesis to produce mutant genes

carrying either the S45A or the Y43A mutations, with an SSGSGSA peptide linker between the SAv and the scFv genes in each construct. The residue changes in fusion genes were determined by DNA sequencing analysis, and the gene products were analyzed by mass spectroscopy, which indicated all FPs differed only at the deliberately engineered positions without any extraneous mutations (data not shown). *E. coli* XL1 Blue (Stratagene) transformants of the gene constructs, WT-SAv, S45A-SAv, or Y43A-SAv, were grown in shaker flasks under control of an IPTG inducible lac promoter for qualitative expression of the FPs. A 4 L fermentor (BioFlo 3000; New Brunswick Scientific) was used for bulk production of FPs. The FPs were purified by iminobiotin chromatography as described (18), except that the loading pH was raised from 9.2 to 11 due to the reduced affinities of the mutant FPs for iminobiotin (33–35). Aggregates were reduced to approximately 3% by treatment with 20% dimethyl sulfoxide (DMSO). The eluted FPs were dialyzed against PBS at 4°C overnight and concentrated to 2.0 to 2.3 mg/mL using a YM30 membrane. The final FPs were filter-sterilized and stored in 5% sorbitol at −80°C. A negative control FP (CC49-WT-SAv) that recognizes the TAG 72 antigen expressed on human adenocarcinomas, but not on lymphomas, was prepared similarly.

Pretargeting reagents

A synthetic, dendrimeric CA containing 16 *N*-acetylgalactosamine residues and a single biotin residue per molecule (NAGB) was obtained from Aletheon Pharmaceuticals for use with 1F5-WT-SAv FP, as described previously (35). A bis-biotin-trigalactose (BBTG) CA containing 2 biotin moieties and 3 galactose residues ($C_{127}H_{218}N_{19}O_{51}S_6$) was used for the clearance of mutant-SAv FPs. The syntheses of BBTG CA and DOTA-bis-biotin have been recently described (28).

Radiolabeling of biotin compounds

^{111}In labeling of DOTA-biotin and DOTA-bis-biotin were conducted as published (28). ^{90}Y labeling for therapy was done similarly, using 2 mg/mL DOTA-bis-biotin, 500 mmol/L ammonium acetate pH 5.3 and ^{90}Y heated for 30 minutes at 85°C. After cooling to room temperature, 100 mmol/L DTPA was added.

In vitro characterization

The FPs were analyzed by SDS-PAGE on 4% to 12% Tris-glycine gels (Invitrogen) under nonreducing conditions. The gels were stained with 0.2% Coomassie blue solution and destained in acetic acid-methanol solution. Size-exclusion high-performance liquid chromatography (HPLC) analysis was done on a Zorbax GF-250 column (9.4 × 250 mm, 4 μm; Agilent) with 20 mmol/L sodium phosphate/0.5 mol/L sodium chloride/15% DMSO (pH 6.8–7.0) as a mobile phase (1 mL/min) and A_{280} as a detection wavelength on a Dynamax system. Matrix-assisted laser desorption/ionization (MALDI) mass spectrometry done on a Voyager DE Pro MALDI time-of-flight mass spectrometer (Applied Biosystems) was used to ascertain the molecular weight of the FPs. The CD20 binding ability of the FPs was assessed using PE-biotin labeled FPs and Ramos target cells. Cells (0.1×10^6 per sample) were incubated with 30 μL of 10 μg/mL 1F5 (positive control) Ab, HB8181 (non-binding isotype control) Ab, 1F5-Y43A-SAv FP, 1F5-S45A-SAv FP, 1F5-WT-SAv FP, or CC49-WT-SAv FP (negative control) for 30 minutes at 4°C. Cells were washed and incubated with 30 μL 1:64 goat anti-mouse IgG (Fab specific) fluorescein isothiocyanate conjugate (Sigma-Aldrich) in PBS. Cells were washed and fluorescence intensity was measured on a FACS Canto I flow cytometer (BD). An *in vitro* cell-binding assay was also done by incubating Ramos cells (1.0×10^6 per sample) with 25 μL of 20 μg/mL 1F5-Y43A-SAv, 1F5-S45A-SAv, 1F5-WT-SAv, or CC49-WT-SAv FPs in a 96 round bottom ELISA plate at 4°C for 60 minutes. Cells were then washed twice in 200 μL PBS. Next, similar molar amounts of ^{90}Y-DOTA–biotin (100 ng/mL) or ^{90}Y-DOTA–bis-biotin (100 ng/mL) were added to the cells and incubated at 4°C for 60 minutes. Cells were washed twice with PBS. Cells were collected using cotton swabs and ^{90}Y activity measured in a gamma counter.

Blood clearance studies

Three groups of 4 athymic mice each were injected via the tail vein (i.v.) with ^{125}I-1F5-Y43A-SAv or ^{125}I-1F5-S45A-SAv FPs (2.8 nmol) followed 24 hours later by i.v. injection of 5.8 nmol of either NAGB or BBTG CA. Venous sampling was done via the tail vein at serial time points up to 68 hours. ^{125}I was counted on a gamma counter and the percent of the injected dose per gram (%ID/g) of blood was calculated.

Mouse xenograft model

FoxN1^{Nu} athymic female mice (6–8 weeks old) were obtained from Harlan Sprague-Dawley and housed in the FHCRC animal facility after approval of the experimental protocol by the Institutional Animal Care and Use Committee. Some groups of mice were switched to a biotin-deficient diet (Purina Mills) 5 to 6 days prior to PRIT studies. Ramos cells (10×10^6) were injected subcutaneously in the right flank 10 days prior to experiments to produce lymphoma xenografts measuring 6 to 10 mm in diameter. Anti-asialoGM1 antiserum (30 μL, WAKO) was injected 9 days and 6 days prior to FP injection to abrogate natural killer cell activity and prevent spontaneous tumor regressions.

Biodistribution studies

Biodistribution experiments were done using the "double label" method of Pressman by trace labeling the 1F5-SAv FPs with ^{125}I and the biotin moiety with ^{111}In to allow independent assessment of tumor targeting of the FPs and the biotin ligands (36). Groups of 5 mice with similar-sized tumors were injected i.v. with 2.8 nmol (400 μg) of 1F5-WT-SAv, 1F5-Y43A-SAv, or 1F5-S45A-SAv FPs labeled with 20 to 40 μCi (0.74–1.48 MBq) of ^{125}I. Twenty hours later, mice were injected with either 5.8 nmol of NAGB CA (50 μg) followed 4 hours later by 1.2 nmol DOTA-biotin labeled with 20 to 40 μCi (0.74–1.48 MBq) of ^{111}In or with 5.8 nmol of BBTG CA (20 μg) followed 4 hours later by 1.2

nmol of ^{111}In -DOTA-bis-biotin. Blood samples, tumors, and body organs were procured and ^{125}I and ^{111}In activities measured in a dual channel gamma counter, adjusting for crossover between channels (17).

Therapy studies

The therapeutic efficacy of ^{90}Y using various pretargeted approaches was evaluated in groups of 5 to 10 mice. Groups of mice with similar sized, palpable tumors were selected and randomized for the studies. Mice were given 2.8 nmol (400 μg) of 1F5-WT-SAv, 1F5-Y43A-SAv, 1F5-S45A-SAv, or the negative control CC49-WT-SAv followed by 5.8 nmol of either NAGB or BBTG CA 20 hours later. A single dose of 1.2 nmol of either DOTA-biotin or DOTA-bis-biotin labeled with 500 μCi (18.5 MBq) ^{90}Y was administered 4 hours after the CA. Mice were assessed every few days for tumor volume measurements, weight change, and general appearance. Mice were euthanized if xenografts exceeded 10% of total body weight, caused obvious discomfort or impaired ambulation, or if mice lost more than 30% of their baseline body weight.

Toxicity studies

Toxicity studies were done in parallel cohort groups, corresponding to the therapy groups. Mice were monitored for lethargy, poor grooming, weight loss and other behaviors consistent with debility. Blood testing was done 14 days after injection of ^{90}Y, and at the time of euthanasia. Laboratory tests done included the leukocyte and platelet counts, hemoglobin, aspartate aminotransferase (AST), alanine aminotransferase (ALT), creatinine, and blood urea nitrogen (BUN) levels. Age-matched, untreated athymic mice were used for comparisons of hematology and chemistry data.

Results

Expression and purification of WT-SAv and mutant-SAv FPs

All FPs were successfully expressed in the periplasmic space of *E. coli* as soluble stable tetramers with molecular weights of approximately 174 KDa (Fig. 1). Expression levels for the FPs varied, with the S45A-SAv construct

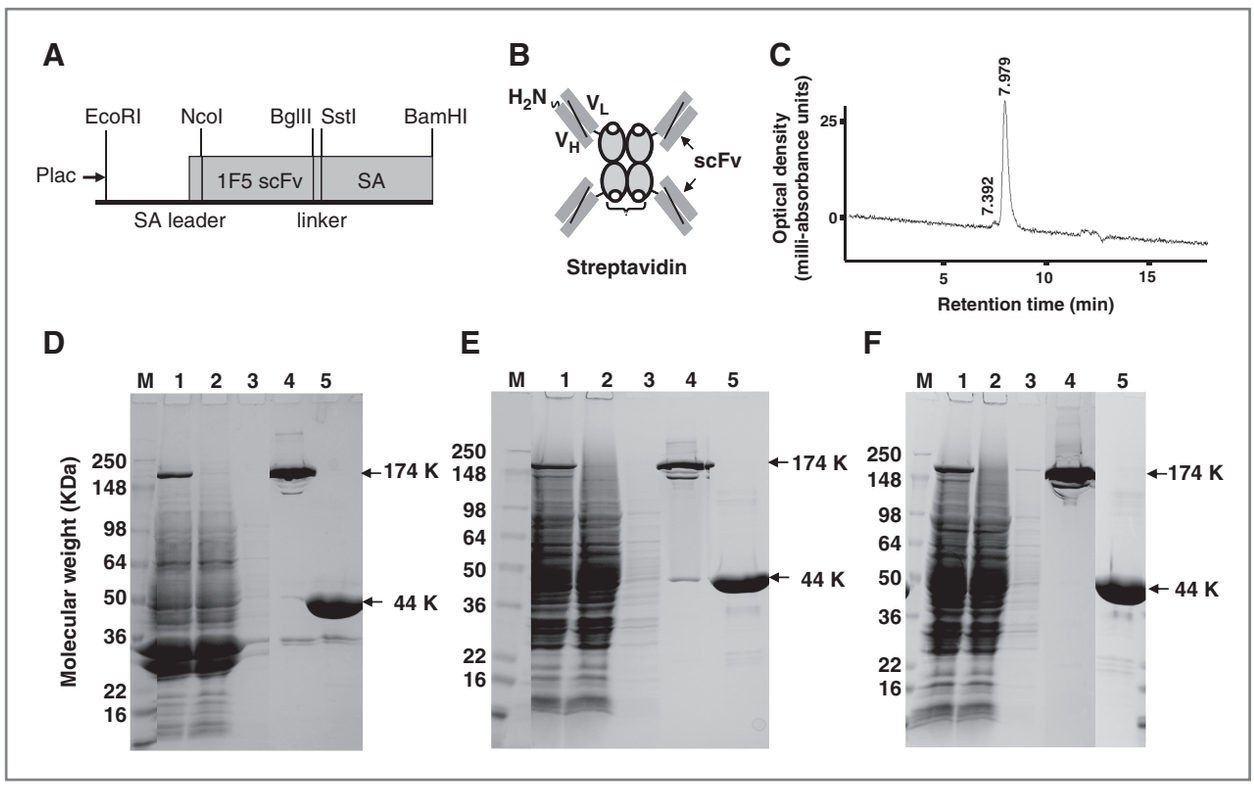

Figure 1. Schematization of the IF5 *scFvSAv* gene and its derivative tetravalent FP. A, the *scFvSAv* fusion gene is comprised of the scFv gene of the murine anti-CD20 1F5 Ab fused to the full length SAv gene. B, a diagrammatic representation of the tetravalent FP that spontaneously forms after secretion into the periplasmic space of *E. coli*. C, representative HPLC tracing of a purified FP (S45A-SA); SDS-PAGE analyses of unpurified and iminobiotin-purified 1F5 $(scFv)_4$SAv WT FP (D), Y43A-SAv FP (E), and S45A-SAv FP (F), respectively. The mass of the intact FPs (174 kDa) and the monomers (44 kDa) are indicated on each SDS-PAGE gels (4%–12% Tris-glycine; Invitrogen) stained with Coomassie blue. Lane M, migration of prestained molecular weight standards (SeeBlue plus; Invitrogen). Lane 1, loaded *E. coli* crude lysate, containing 1F5$(scFv)_4$SAv WT FP. Lanes 2 and 3, flow-through and wash fractions, respectively, from an iminobiotin purification column. Lanes 4 and 5, iminobiotin-purified FP without boiling (lane 4) or denatured by boiling for 5 minutes to resolve the tetramers into monomers (lane 5).

producing the highest yield (358 mg/L), followed by Y43A-SAv (144 mg/L) and WT-SAv (100 mg/L; ref. 18). SDS-PAGE analysis confirmed purities of approximately 95% for the WT-SAv and mutant-SAv FPs after iminobiotin chromatography. All tetrameric FP bands resolved into a single species of MW ~ 44 kDa when the FPs were denatured by boiling before electrophoresis, consistent with a single protein entity dissociable into a homogeneous, monomeric subunit (Fig. 1).

In vitro characterizations of mutant-SAv FPs

Flow cytometry showed similar binding of the WT-SAv, S45A-SAv, and Y43A-SAv FPs and of the parental 1F5 antibody to CD20-expressing Ramos cells (Fig. 2). *In vitro* cell-binding assays were then done to compare the capture and retention of radiolabeled biotin moieties by FPs bound to CD20 on the surface of lymphoma cells (Fig. 3). As expected, the engineered low-affinity mutant FPs, 1F5-S45A-SAv and 1F5-Y43A-SAv, bound significantly less radiolabeled monovalent biotin (2.9 ± 0.003% and 4.9 ± 0.010% of the total ^{90}Y activity presented to the cells, respectively) than did the WT-SAv FP (12.1 ± 0.02% of the ^{90}Y activity added to the cultures). S45A-SAv and Y43A-SAv FPs were much more successful, as designed, in binding and retaining radiolabeled divalent bis-biotin (18.1 ± 0.005% and 17.4 ± 0.001% of applied ^{90}Y activity, respectively). By comparison, WT-SAv FP bound 25.6 ± 0.02% of applied ^{90}Y-labeled divalent bis-biotin. These results show that the divalent binding of the bis-biotin ligand compensated for the lower affinity of the Y43A and S45A mutant SAv molecules, yielding binding pairs at least comparable with the standard WT-SAv and monovalent DOTA-biotin reagents.

Blood clearance studies

The blood clearances of ^{125}I-labeled mutant-SA FPs were evaluated after administration of CAs to athymic mice fed biotin-replete normal diets. Groups of 4 mice each were given 2.8 nmol of S45A-SAv or Y43A-SAv FP followed 20 hours later by divalent BBTG CA, monovalent NAGB CA, or PBS (negative control). A single injection of 5.8 nmol BBTG CA resulted in an approximately 80% decrease of circulating ^{125}I-1F5-S45A-SAv within 30 minutes (shown logarithmically in Fig. 4) and an approximately 60% decrease in ^{125}I-1F5-Y43A-SAv (not shown). In contrast, the monovalent biotin CA, NAGB, was ineffective at clearing the low affinity ^{125}I-1F5-S45A-SAv or ^{125}I-1F5-Y43A-SAv FPs from the blood, with clearances not significantly different from those seen in negative control mice treated with PBS (Fig. 4). These results show that the bis-biotin BBTG CA we designed works effectively as planned for the low affinity FPs, but that the standard NAGB CA, which possesses only a single biotin moiety, is ineffective for these constructs.

Biodistribution studies

Biodistribution experiments were conducted in mice with 1F5-Y43A-SAv, 1F5-S45A-SAv, and 1F5-WT-SAv FPs and biotin compounds using the "dual label" method described previously. Groups of 5 athymic mice-bearing Ramos xenografts were injected i.v. with 400 μg (2.8 nmol) of ^{125}I-labeled WT-SAv, Y43A-SAv, or S45A-SAv FPs followed 20 hours later by 5.8 nmol of BBTG or NAGB CA. Four hours later, mice were injected i.v. with 1.2 nmol of ^{111}In-DOTA-bis-biotin or ^{111}In-DOTA-biotin. Mice were euthanized 24 hours (Fig. 5A) or 48 hours (Fig. 5B) later and ^{125}I and ^{111}In were measured in excised tumors and normal organs using a dual channel gamma counter, adjusting for crossover of the 2 isotopes between channels. Biodistributions using the mutant-SA FPs did not include groups of mice on biotin-deficient diets because previous studies showed no differences in tumor uptake between mice on biotin-deficient

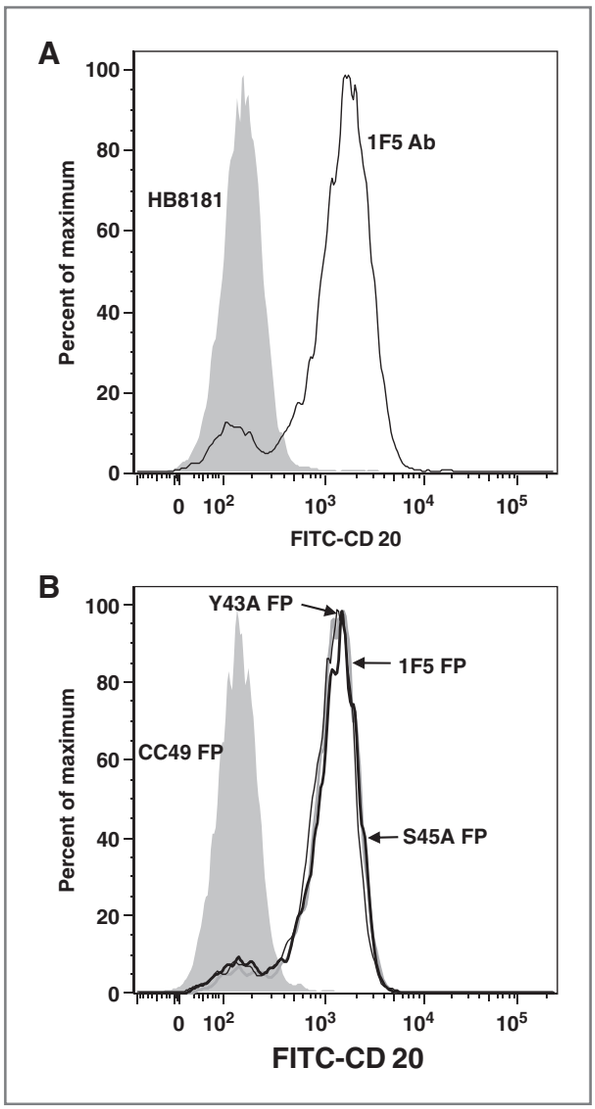

Figure 2. Flow cytometry showing equivalent binding of the 1F5-WT-SAv, 1F5-Y43A-SAv, and 1F5-S45A-SAv FPs to the surface of CD20-expressing Ramos cells (B). For comparison, binding of a nonbinding negative control FP, CC49-WT-SAv (B), a nonbinding, isotype matched, negative control Ab, HB8181 (A), and the parental 1F5 anti-CD20 Ab (positive control, A) are also shown.

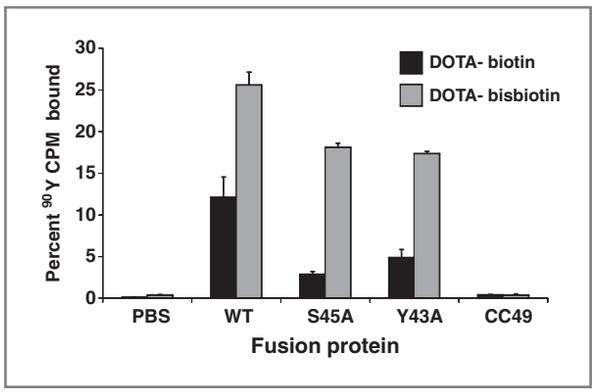

Figure 3. Cell-binding assay comparing the binding of ^{90}Y-DOTA-biotin and ^{90}Y-DOTA-bis-biotin to Ramos cells previously saturated with 1F5-WT-SAv FP, 1F5-Y43A-SAv FP, 1F5-S45A-SAv FP, or CC49-SA FP (negative control) or to untreated cells incubated with PBS. Ramos cells (1.0×10^6 per sample) were incubated with 25 μL of 20 μg/mL 1F5-Y43A-SAv, 1F5-S45A-SAv, 1F5-WT-SAv, or CC49-WT-SAv FPs in a 96 round bottom ELISA plate at 4°C for 60 minutes. Cells were then washed twice in PBS. Next, 100 ng/mL of ^{90}Y-DOTA–biotin or ^{90}Y-DOTA–bis-biotin was added to the cells and incubated at 4°C for 60 minutes. Cells were washed twice with PBS and then bound radioactivity was measured in a gamma counter.

diets and normal diets with mutant sAv conjugates (29). There were no significant differences in tumor or normal organ biodistributions of ^{125}I in groups given mutant-SAv or WT-SAv FPs at either 24 or 48 hours, indicating that all the anti-CD20 FPs have similar tumor targeting and tissue biodistributions (Supplementary Fig. S1). Analyses of the biodistributions of ^{111}In-labeled biotin compounds indicated that ^{111}In-DOTA-bis-biotin was effectively targeted to tumors in mice pretargeted with mutant-SAv FPs even when mice were fed normal biotin-containing diets, whereas monovalent ^{111}In-DOTA–biotin was not effectively targeted to lymphoma xenografts with the standard WT-SAv FP unless mice were fed rigorously restricted biotin-free diets (Fig. 5). Tumors from mice pretargeted with Y43A-SAv FP followed by ^{111}In-DOTA-bis-biotin contained 6.2 ± 1.7% of the injected ^{111}In per gram of tumor (%ID/gm) after 24 hours compared with 5.6 ± 2.2%ID/g with S45A-SAv but only 2.5 ± 1.6%ID/g with WT-SAv FP ($P = 0.01$; Fig. 5A). The amount of radioactivity in tumors of mice treated with the mutant FP/bis-biotin systems were similar to the radioactivity in tumors excised from mice fed a biotin-deficient diet and treated with the standard WT-SAv FP and DOTA-biotin PRIT system (7.2 ± 3.2%ID/g after 24 hours, $P > 0.3$). Similar conclusions were derived from biodistribution studies conducted 48 hours after injection of ^{111}In-labeled biotin compounds (Fig. 5B). Tumors excised from mice on normal diets treated with the mutant-SAv FPs followed by ^{111}In-DOTA-bis-biotin contained 4.6 ± 1.0%ID/g of the injected ^{111}In- DOTA-bis-biotin with Y43A-SAv FP and 3.6 ± 1.1%ID/g with S45A-SAv FP after 48 hours compared with 1.1 ± 0.3%ID/g with WT-SAv FP (Fig. 6B; $P < 0.0001$). Tumors from mice fed a biotin-deficient diet and treated with WT-SAv FP and monovalent ^{111}In-DOTA-biotin contained 5.2 ± 0.4%ID/g after 48 hours. The biodistributions of ^{111}In-DOTA-bis-biotin and ^{111}In-DOTA-biotin in normal organs were similar in mice treated with either mutant-SAv FPs or WT-SAv FP, except that radioactivity in the blood and liver were slightly higher with mutant-SAv FPs, especially for Y43A-SAv (Fig. 5). The amount of radioactivity measured in tumors of mice fed normal diets treated with WT-SAv FP did not vary significantly whether ^{111}In-DOTA- biotin or ^{111}In-DOTA-bis-biotin was used, indicating that even the bis-biotin ligand was not able to displace prebound endogenous biotin from the biotin-binding sites of WT-SAv. Overall, the combination of mutant-SAv FPs, BBTG CA, and DOTA-bis-biotin resulted in superior biodistributions of radioactivity compared with conventional WT-SAv FP, NAGB CA, and DOTA-biotin in mice fed normal diets, where endogenous biotin levels are known to be high.

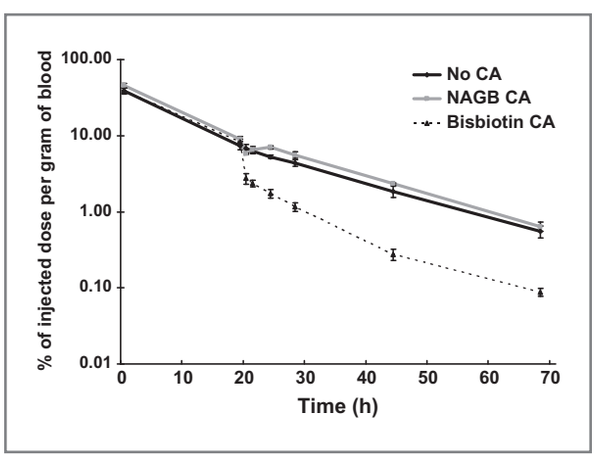

Figure 4. Blood clearance of ^{125}I-1F5-S45A-SA FP using either a monovalent biotin CA (NAGB, ◆) or a synthetic bis-biotin CA (BBTG-CA, ▲). CAs (5.8 nmol) were injected 20 hours after administration of FP, then mice were bled serially and blood radioactivity measured in a gamma counter. Control mice received 2.8 nmol of FPs without any CA (●). Results are expressed as the percent of the injected dose of radioactivity present per gram of blood (%ID/g) on a logarithmic scale.

Therapy and toxicity studies

Therapy studies compared the efficacy of ^{90}Y-labeled biotin compounds for treating lymphoma xenografts in mice pretargeted with the WT and mutant SAv FPs or with a nonbinding negative control, CC49-WT-SAv FP (Fig. 6). Mice were assigned into 6 different groups and fed either a biotin-deficient diet or a regular biotin-containing diet. The median tumor size was 86 ± 42 mm^3 at the initiation of the study with no significant differences between groups. Mice were treated with WT-SAv, S45A-SAv, Y43A-SAv, or CC49-WT-SAv FPs followed 20 hours later by either NAGB or BBTG CA. A single injection of 500 μCi [^{90}Y]-labeled DOTA-bis-biotin or monovalent DOTA-biotin was given 4 hours after the CA injection. Animals on a regular diet that received Y43A-SAv and S45A-SAv FPs had mean tumor volumes of 236 ± 66 mm^3 and 543 ± 320 mm^3 11 days after therapy, respectively, compared with 1435 ± 212 mm^3 for mice that received a nonbinding

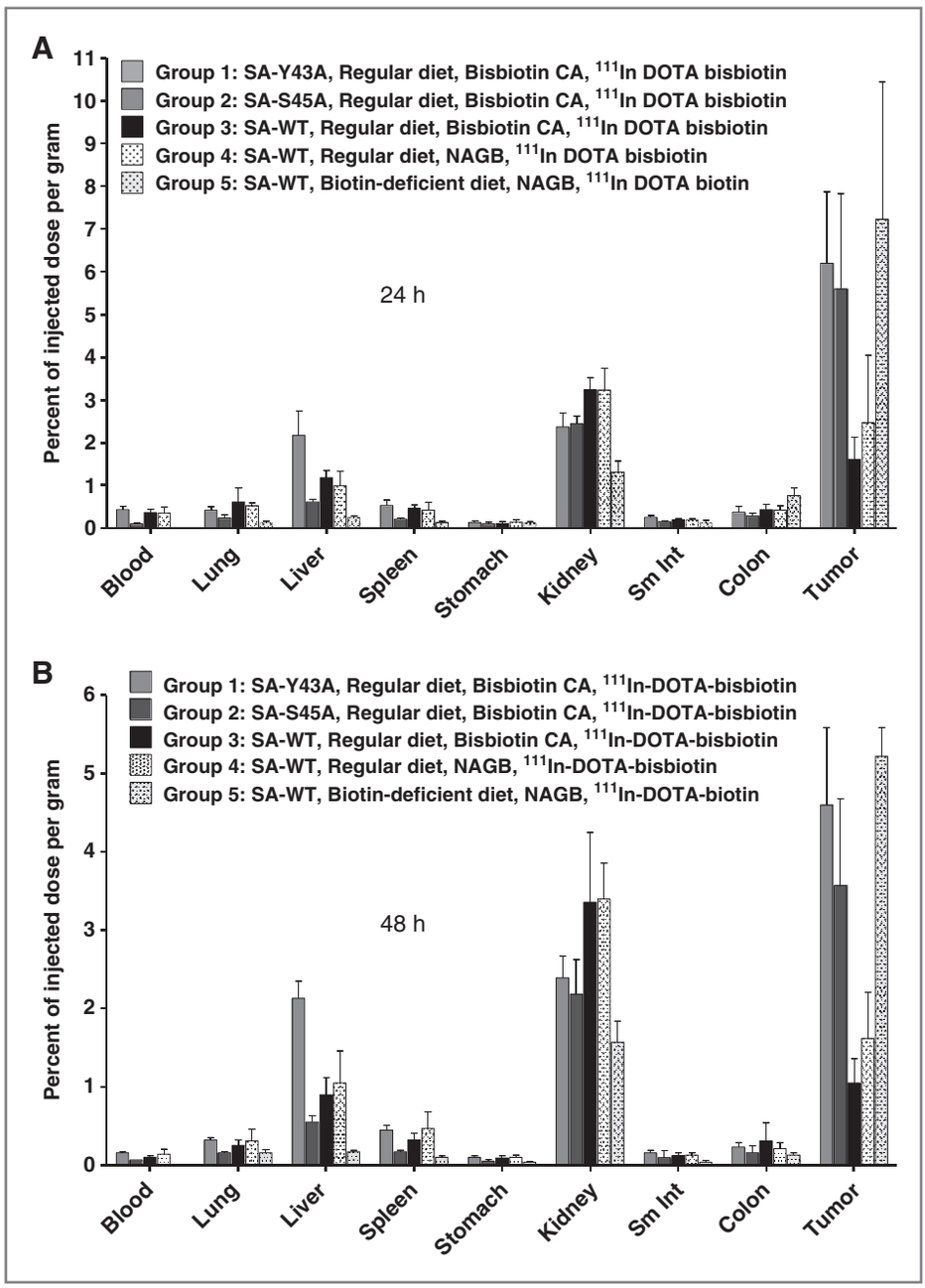

Figure 5. Biodistributions of ^{111}In-labeled biotin compounds in tumors and normal organs of athymic mice-bearing Ramos xenografts pretargeted with 1F5-S45A-SAv, 1F5-Y43A-SAv, or 1F5-WT-SAv FP. Mice were fed either normal or biotin-deficient diets for 5 to 6 days before injection of 2.8 nmol of FPs, as indicated. Twenty-four hours later, 5.8 nmol of either monovalent NAGB CA or divalent bis-biotin CA was injected. After another 4 hours, mice were injected with 1.2 nmol of ^{111}In-labeled DOTA-biotin or ^{111}In-labeled bis-biotin. Results are shown for mice sacrificed either 24 hours (A) or 48 hours (B) after administration of the radiolabeled biotin ligands.

control CC49-SAv FP ($P < 0.0001$) and 1129 ± 322 mm^3 for animals that received WT-SAv FP ($P < 0.03$). Administration of WT-SAv FP to mice fed a biotin-deficient diet was associated with the most significant delay in tumor growth (11 ± 22 mm^3 at day 11). Treatment was well tolerated with no evidence of acute toxicity. Complete blood counts, creatinine, and transaminase levels 14 days after therapy were similar in all groups of mice except that mildly lower leukocyte counts were observed in mice in all of the treatment groups compared with control, untreated mice (Supplementary Table S2).

Discussion

The efficacy of RIT in patients with NHL has been established by a multitude of clinical trials, but the majority of patients treated with nonmyeloablative doses of RIT eventually relapse (37–38). PRIT using SAv-biotin methodology has emerged as one promising approach to deliver potentially curative radiation doses to tumors while minimizing toxicities arising from the nonspecific radiation delivered to normal organs. Although the high affinity of SAv for biotin is essential for this pretargeting system, this tight interaction

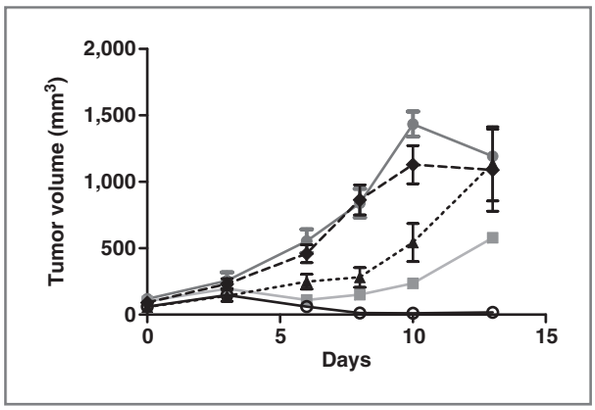

Figure 6. Growth of Ramos xenografts in athymic mice pretargeted with CC49-SAv FP (nonbinding negative control, ●), 1F5-S45A-SAv FP (▲), 1F5-Y43A-SA FP (■), 1F5-WT-SAv (◆), or 1F5-WT-SAv with a biotin-deficient diet (●) followed by the indicated CA and ^{90}Y-DOTA-bisbiotin or ^{90}Y-DOTA-biotin. Mice were fed a normal, biotin-replete diet unless otherwise specified.

can paradoxically present a significant limitation when naturally occurring endogenous biotin irreversibly blocks the SAv-binding sites, decreases the capacity of SAv to bind radiolabeled DOTA-biotin, and reduces therapeutic efficacy. Although short-term biotin-depletion can be routinely achieved in mouse models, rigorous biotin-depletion is difficult in clinical settings due to its ubiquitous presence in all common foods. Even if endogenous biotin is successfully depleted, suboptimal targeting may still occur because the extremely slow "off rate" of radiobiotin hinders its diffusion to the center of tumor masses, due to "trapping" of radiobiotin in perivascular or peripheral locations by irreversible, high-affinity binding to the most accessible tumor cells. Computer models and experimental data have verified that such a "binding-site barrier" does exist and may compromise therapeutic efficacy of radioimmunoconjugates of extremely high-binding affinities, though this problem can be at least partially overcome by administration of a large excess of Ab-SAv conjugate and radiobiotin (39–40). In this study, we show the potential advantage of a novel, engineered PRIT system utilizing mutant-SAv FPs and bivalent radiolabeled DOTA-bis-biotin for treatment of lymphomas in situations where endogenous biotin may limit the effectiveness of standard SAv-biotin PRIT. Our group has previously shown that specific delivery of high doses of radiation to tumor sites is achievable even in the presence of endogenous biotin using chemical conjugates of 1F5 Ab and mutant-SAv protein produced using heterobifunctional cross-linkers in combination with bivalent biotin ligands (28–29). Here, we describe the genetic engineering, expression, *in vitro* characterization, and *in vivo* testing of novel 1F5-mutant-SAv FPs, which are more homogeneous, more amenable to scale-up, and less costly to manufacture than the previously described Ab-mutant-SAv chemical conjugates (33).

We have produced anti-CD20 mutant-SAv FPs that maintain the full antigen-binding capacity of the parent monoclonal Ab, but have a reduced avidity for endogenous biotin compared with WT-SAv FP. We selected the Y43A and S45A mutants for incorporation into $scFv_4$SAv FPs from a panel of available mutants produced by site-directed mutagenesis based on prior *in vitro* assays, which suggested that these particular mutations would be most advantageous (27, 29). The Y43A-SAv and S45A-SAv mutant molecules have 67- and 907-fold lower affinity for biotin, respectively, compared with WT-SAv, but retain robust binding to divalent biotin compounds, as shown by their significantly slower off-rates for bis-biotin than biotin (27). Mutant-SAv FPs were directly compared with WT-SAv FP using a cell-binding assay (Fig. 3), which showed that both Y43A-SAv and S45A-SAv FPs have significantly lower affinity for monovalent biotin compared with WT-SAv FP, but have sufficiently high affinity to efficiently capture bis-biotin ligands. These *in vitro* results suggest that the lower affinity of the mutant-SAv FPs for monovalent biotin may allow prebound endogenous monovalent biotin to quickly dissociate, yet permit the durable capture and retention of radiolabeled divalent bis-biotin ligands by mutant-SAv FPs. To utilize this mutant-SAv FP and bis-biotin system effectively, a synthetic trigalactose-containing bis-biotin CA was conceptualized and generated by our group to facilitate blood clearance of the mutant-SAv FPs (28). Pharmacokinetic experiments showed that treatment of mice with BBTG CA resulted in efficient clearance of mutant-SAv FPs from the blood. As expected, the standard CA containing a single biotin moiety (NAGB) had a negligible effect on the blood clearance of the mutant-SAv FPs.

Biodistribution experiments confirmed that the uptake and retention of radiolabeled DOTA-biotin by WT-SAv FP was significantly compromised at tumor sites when animals were fed a regular diet, presumably because of the deleterious impact of endogenous biotin blocking the biotin-binding sites of SAv. In marked contrast, the mutant-SAv FPs exhibited excellent tumor retention of radiolabeled DOTA-bis-biotin even in animals fed a regular biotin-rich diet. The amounts of radioactivity in normal tissues were similar in mice treated with mutant-SAv and WT-SAv FPs, except for the blood and liver, which contained slightly more radioactivity in groups treated with mutant-SAv than in mice treated with WT-SAv and NAGB CA. We presume these differences emerged because the BBTG CA was less efficient at clearing mutant-SAv FPs from the blood than the NAGB CA was at clearing WT-SAv (17, 41). Therefore, further optimization of the bis-biotin CA is planned using variations in the galactose content of the molecule.

In therapy experiments, mutant-SAv FPs in combination with ^{90}Y-DOTA-bis-biotin produced significant tumor growth delays in mice bearing lymphoma xenografts fed biotin-replete normal diets while the standard regimen, utilizing WT-SAv and ^{90}Y-DOTA-biotin, had no significant effect on tumor growth in the presence of endogenous biotin. These data support the hypothesis that mutant-SAv FPs with optimized biotin-binding affinities can improve the amount of radiation delivered specifically to tumor sites

compared with WT-SAv FP in the presence of competing endogenous biotin.

Although it must be acknowledged that the current gold standard combination of WT-SA FP and radiolabeled DOTA-biotin remains superior in situations where rigorous biotin depletion can be achieved, these studies show the promise of such a genetically engineered PRIT system for situations where endogenous biotin may limit its efficacy through competitive inhibition at the SAv-binding site. In addition, it is conceivable that the SAv mutants used in these experiments may not possess the optimal off-rates for biotin and bis-biotin to maximize tumor retention. Therefore, additional mutant-SAv FPs will be engineered and tested to further optimize the affinity and off-rate for monovalent biotin and bivalent biotin ligands.

We acknowledge that one potential limitation of SAv-biotin pretargeting systems is the immunogenicity of SAv (and of murine Ab). Although human anti-mouse Ab (HAMA) and human anti-SAv Ab (HASA) may be major limitations for applications in immunocompetent patients and for experimental regimens requiring repetitive rounds of therapy, we do not anticipate that immunogenicity will be a major limitation for this approach in patients with advanced leukemia and lymphoma, who are the focus of our investigations. We have administered RIT using murine Ab to 476 patients with non-Hodgkin lymphoma or acute myeloid leukemia at our center since 1987. Only 14 of these 476 patients (2.9%) formed HAMA between the dosimetric and therapeutic infusions of radiolabeled Ab. Furthermore, we recently opened a clinical trial of PRIT using a murine anti-CD45 Ab with SAv and radiolabeled biotin for patients with acute myeloid leukemia (ClinicalTrials.gov identifier NCT00988715; IND # 104683). No immune responses to either Ab or SAv have yet been detected in the 5 patients treated, presumably due to the compromised immune system of these patients (unpublished data). HASA have also not been major impediments in published studies of lymphoma patients treated with streptavidin-biotin PRIT by others (19, 22). We believe that our ongoing trial, and previous PRIT studies by others, show that Ab-SA PRIT approaches are translatable to the clinic.

In summary, we have shown the potential of rationally engineered mutant-SAv FPs to be used in conjunction with divalent bis-biotin CA and bis-biotin radioisotope carriers to circumvent the potential blocking effects of endogenous biotin. This approach may allow the effective delivery of higher doses of radiation to tumor sites than is possible with standard SAv-biotin PRIT systems in settings where rigorous biotin depletion is not feasible.

Disclosure of Potential Conflicts of Interest

O.W. Press has received honoraria for consultation from Algeta, Roche/Genentech, Spectrum Pharmaceuticals, and Seattle Genetics and research support from Roche/Genentech. A.K. Gopal has received honoraria for lectures from Seattle Genetics and Millennium and research support from Glaxo Smith Kline, Merck, Cephalon, Piramal, Pfizer, Abbott, BioMarin, Seattle Genetics, Eli Lilly, and Spectrum Pharmaceuticals. J.M. Pagel has research support from Glaxo Smith Kline. The other authors disclosed no potential conflicts of interest.

Authors' Contributions

S.I. Park designed and performed research, analyzed data, and drafted the manuscript. J. Shenoi designed and performed research, analyzed data, and drafted the manuscript. S. Frayo performed research, collected data, and analyzed data. D.K. Hamlin contributed vital reagents and performed research. Y. Lin engineered, expressed, purified, and tested the fusion proteins. P.S. Stayton produced the mutant streptavidin gene constructs by directed mutagenesis. D.S. Wilbur contributed to the conception, design, analysis, and interpretation of research. N. Orgun, A. Kenoyer, and A. Axtman performed research and collected data. M. Hylarides contributed vital reagents, design and interpretation of research. F. Buchegger performed research and analyzed data. A.K. Gopal and D.J. Green contributed to the interpretation of data. J.M. Pagel contributed to the conception, design, analysis, and interpretation of research and edited the manuscript. O.W. Press contributed to the conception, design, analysis and interpretation of research, revised the manuscript, and funded the experiments.

Grant Support

This work was supported by grants from the NIH: RO1 CA076287, PO1 CA44991, and the Lymphoma Research Foundation and gifts from David and Patricia Giuliani, Mary and Geary Britton-Simmons, James and Sherry Raisbeck, the Wyner-Stokes Foundation, and the Hext Family Foundation. A.K. Gopal is a scholar in clinical research of the Leukemia and Lymphoma Society. S.I. Park is a recipient of a Lymphoma Research Foundation Fellowship Award.

The costs of publication of this article were defrayed in part by the payment of page charges. This article must therefore be hereby marked *advertisement* in accordance with 18 U.S.C. Section 1734 solely to indicate this fact.

Received May 10, 2011; revised July 23, 2011; accepted September 21, 2011; published OnlineFirst October 5, 2011.

References

1. Vose JM. Current approaches to the management of non-Hodgkin's lymphoma. Semin Oncol 1998;25:483–91.
2. Fisher RI, Gaynor ER, Dahlberg S, Oken MM, Grogan TM, Mize EM, et al. Comparison of a standard regimen (CHOP) with three intensive chemotherapy regimens for advanced non-Hodgkin's lymphoma. N Engl J Med 1993;328:1002–6.
3. Horning SJ. Treatment approaches to the low-grade lymphomas. Blood 1994;83:881–4.
4. Kaminski MS, Zelenetz AD, Press OW, Saleh M, Leonard J, Fehrenbacher L, et al. Pivotal study of iodine I 131 tositumomab for chemotherapy-refractory low-grade or transformed low-grade B-cell non-Hodgkin's lymphomas. J Clin Oncol 2001;19:3918–28.
5. Knox SJ, Goris ML, Trisler K, Negrin R, Davis T, Liles TM, et al. Yttrium-90-labeled anti-CD20 monoclonal antibody therapy of recurrent B-cell lymphoma. Clin Cancer Res 1996;2:457–70.
6. Witzig TE, Gordon LI, Cabanillas F, Czuczman MS, Emmanouilides C, Joyce R, et al. Randomized controlled trial of yttrium-90-labeled ibritumomab tiuxetan radioimmunotherapy versus rituximab immunotherapy for patients with relapsed or refractory low-grade, follicular, or transformed B-cell non-Hodgkin's lymphoma. J Clin Oncol 2002;20:2453–63.
7. Vose JM, Wahl RL, Saleh M, Rohatiner AZ, Knox SJ, Radford JA, et al. Multicenter phase II study of iodine-131 tositumomab for chemotherapy-relapsed/refractory low-grade and transformed

low-grade B-cell non-Hodgkin's lymphomas. J Clin Oncol 2000;18: 1316–23.
8. Gopal AK, Gooley TA, Maloney DG, Petersdorf SH, Eary JF, Rajendran JG, et al. High-dose radioimmunotherapy versus conventional high-dose therapy and autologous hematopoietic stem cell transplantation for relapsed follicular non-Hodgkin lymphoma: a multivariable cohort analysis. Blood 2003;102:2351–7.
9. Press OW, Eary JF, Appelbaum FR, Martin PJ, Badger CC, Nelp WB, et al. Radiolabeled-antibody therapy of B-cell lymphoma with autologous bone marrow support. N Engl J Med 1993;329:1219–24.
10. Press OW, Eary JF, Gooley T, Gopal AK, Liu S, Rajendran JG, et al. A phase I/II trial of iodine-131-tositumomab (anti-CD20), etoposide, cyclophosphamide, and autologous stem cell transplantation for relapsed B-cell lymphomas. Blood 2000;96:2934–42.
11. Goodwin DA, Meares CF, Osen M. Biological properties of biotin-chelate conjugates for pretargeted diagnosis and therapy with the avidin/biotin system. J Nucl Med 1998;39:1813–8.
12. Rosebrough SF. Pharmacokinetics and biodistribution of radiolabeled avidin, streptavidin and biotin. Nucl Med Biol 1993;20:663–8.
13. Paganelli G, Malcovati M, Fazio F. Monoclonal antibody pretargetting techniques for tumour localization: the avidin-biotin system. International Workshop on Techniques for Amplification of Tumour Targetting. Nucl Med Commun 1991;12:211–34.
14. Goodwin DA, Meares CF. Advances in pretargeting biotechnology. Biotechnol Adv 2001;19:435–50.
15. Hnatowich DJ, Virzi F, Rusckowski M. Investigations of avidin and biotin for imaging applications. J Nucl Med 1987;28:1294–302.
16. Axworthy DB, Reno JM, Hylarides MD, Mallett RW, Theodore LJ, Gustavson LM, et al. Cure of human carcinoma xenografts by a single dose of pretargeted yttrium-90 with negligible toxicity. Proc Natl Acad Sci U S A 2000;97:1802–7.
17. Press OW, Corcoran M, Subbiah K, Hamlin DK, Wilbur DS, Johnson T, et al. A comparative evaluation of conventional and pretargeted radioimmunotherapy of CD20-expressing lymphoma xenografts. Blood 2001;98:2535–43.
18. Pagel JM, Lin Y, Hedin N, Pantelias A, Axworthy D, Stone D, et al. Comparison of a tetravalent single-chain antibody-streptavidin fusion protein and an antibody-streptavidin chemical conjugate for pretargeted anti-CD20 radioimmunotherapy of B-cell lymphomas. Blood 2006;108:328–36.
19. Forero A, Weiden PL, Vose JM, Knox SJ, LoBuglio AF, Hankins J, et al. Phase 1 trial of a novel anti-CD20 fusion protein in pretargeted radioimmunotherapy for B-cell non-Hodgkin lymphoma. Blood 2004;104: 227–36.
20. Forero-Torres A, Shen S, Breitz H, Sims RB, Axworthy DB, Khazaeli MB, et al. Pretargeted radioimmunotherapy (RIT) with a novel anti-TAG-72 fusion protein. Cancer Biother Radiopharm 2005;20: 379–90.
21. Knox SJ, Goris ML, Tempero M, Weiden PL, Gentner L, Breitz H, et al. Phase II trial of yttrium-90-DOTA-biotin pretargeted by NR-LU-10 antibody/streptavidin in patients with metastatic colon cancer. Clin Cancer Res 2000;6:406–14.
22. Weiden PL, Breitz HB, Press O, Appelbaum JW, Bryan JK, Gaffigan S, et al. Pretargeted radioimmunotherapy (PRIT) for treatment of non-Hodgkin's lymphoma (NHL): initial phase I/II study results. Cancer Biother Radiopharm 2000;15:15–29.
23. Baker H. Assessment of biotin status: clinical implications. Ann N Y Acad Sci 1985;447:129–32.
24. Shriver BJ, Roman-Shriver C, Allred JB. Depletion and repletion of biotinyl enzymes in liver of biotin-deficient rats: evidence of a biotin storage system. J Nutr 1993;123:1140–9.
25. Stayton PS, Nelson KE, McDevitt TC, Bulmus V, Shimoboji T, Ding Z, et al. Smart and biofunctional streptavidin. Biomol Eng 1999; 16:93–9.
26. Freitag S, Le Trong I, Chilkoti A, Klumb LA, Stayton PS, Stenkamp RE. Structural studies of binding site tryptophan mutants in the high-affinity streptavidin-biotin complex. J Mol Biol 1998;279:211–21.
27. Hamblett KJ, Kegley BB, Hamlin DK, Chyan MK, Hyre DE, Press OW, et al. A streptavidin-biotin binding system that minimizes blocking by endogenous biotin. Bioconjug Chem 2002;13:588–98.
28. Wilbur DS, Park SI, Chyan MK, Wan F, Hamlin DK, Shenoi J, et al. Design and synthesis of bis-biotin-containing reagents for applications utilizing monoclonal antibody-based pretargeting systems with streptavidin mutants. Bioconjug Chem 2010;21:1225–38.
29. Hamblett KJ, Press OW, Meyer DL, Hamlin DK, Axworthy D, Wilbur DS, et al. Role of biotin-binding affinity in streptavidin-based pretargeted radioimmunotherapy of lymphoma. Bioconjug Chem 2005; 16:131–8.
30. Wilbur DS, Chyan MK, Pathare PM, Hamlin DK, Frownfelter MB, Kegley BB. Biotin reagents for antibody pretargeting. 4. Selection of biotin conjugates for *in vivo* application based on their dissociation rate from avidin and streptavidin. Bioconjug Chem 2000;11:569–83.
31. Wilbur DS, Pathare PM, Hamlin DK, Weerawarna SA. Biotin reagents for antibody pretargeting. 2. Synthesis and *in vitro* evaluation of biotin dimers and trimers for cross-linking of streptavidin. Bioconjug Chem 1997;8:819–32.
32. Wilbur DS, Hamlin DK, Chyan MK, Kegley BB, Pathare PM. Biotin reagents for antibody pretargeting. 5. Additional studies of biotin conjugate design to provide biotinidase stability. Bioconjug Chem 2001;12:616–23.
33. Lin Y, Pagel JM, Axworthy D, Pantelias A, Hedin N, Press OW. A genetically engineered anti-CD45 single-chain antibody-streptavidin fusion protein for pretargeted radioimmunotherapy of hematologic malignancies. Cancer Res 2006;66:3884–92.
34. Klumb LA, Chu V, Stayton PS. Energetic roles of hydrogen bonds at the ureido oxygen binding pocket in the streptavidin-biotin complex. Biochemistry 1998;37:7657–63.
35. Schultz J, Lin Y, Sanderson J, Zuo Y, Stone D, Mallett R, et al. A tetravalent single-chain antibody-streptavidin fusion protein for pretargeted lymphoma therapy. Cancer Res 2000;60:6663–9.
36. Pressman D. Radiolabeled antibodies. Ann N Y Acad Sci 1957;69: 644–50.
37. Gordon LI, Molina A, Witzig T, Emmanouilides C, Raubtischek A, Darif M, et al. Durable responses after ibritumomab tiuxetan radioimmunotherapy for CD20+ B-cell lymphoma: long-term follow-up of a phase 1/2 study. Blood 2004;103:4429–31.
38. Fisher RI, Kaminski MS, Wahl RL, Knox SJ, Zelenetz AD, Vose JM, et al. Tositumomab and iodine-131 tositumomab produces durable complete remissions in a subset of heavily pretreated patients with low-grade and transformed non-Hodgkin's lymphomas. J Clin Oncol 2005;23:7565–73.
39. Sung C, van Osdol WW, Saga T, Neumann RD, Dedrick RL, Weinstein JN. Streptavidin distribution in metastatic tumors pretargeted with a biotinylated monoclonal antibody: theoretical and experimental pharmacokinetics. Cancer Res 1994;54:2166–75.
40. Fujimori K, Covell DG, Fletcher JE, Weinstein JN. A modeling analysis of monoclonal antibody percolation through tumors: a binding-site barrier. J Nucl Med 1990;31:1191–8.
41. Pagel JM, Hedin N, Subbiah K, Meyer D, Mallet R, Axworthy D, et al. Comparison of anti-CD20 and anti-CD45 antibodies for conventional and pretargeted radioimmunotherapy of B-cell lymphomas. Blood 2003;101:2340–8.